New half-lives and beta-delayed neutron branchings for neutron-rich Ba to Nd nuclei (A~160) relevant for the formation of the r-process rare-earth peak

M. Pallàs[1], A. Tarifeño-Saldivia[2,1], A. Tolosa-Delgado[3,2], G. G. Kiss[4], J. L. Tain[2], A. Vitéz-Sveiczer[4] for the BRIKEN collaboration[5]

[1]Institut de Tècniques Energètiques (INTE), Universitat Politècnica de Catalunya (UPC), Barcelona, Spain
[2]Instituto de Física Corpuscular (IFIC), Paterna, Spain
[3]European Organization for Nuclear Research (CERN), Geneva, Switzerland
[4]Institute for Nuclear Research (ATOMKI), Debrecen, Hungary
[5]www.wiki.edu.ac.uk/display/BRIKEN/Home

Index

1. Introduction and motivation
2. Experimental setup
3. Analysis methodology
4. Experimental results

Motivation

r-process (rapid neutron capture)

1. Neutron rich region
2. Timescale us-ms
3. Responsible for around half of the nuclei heavier than iron.

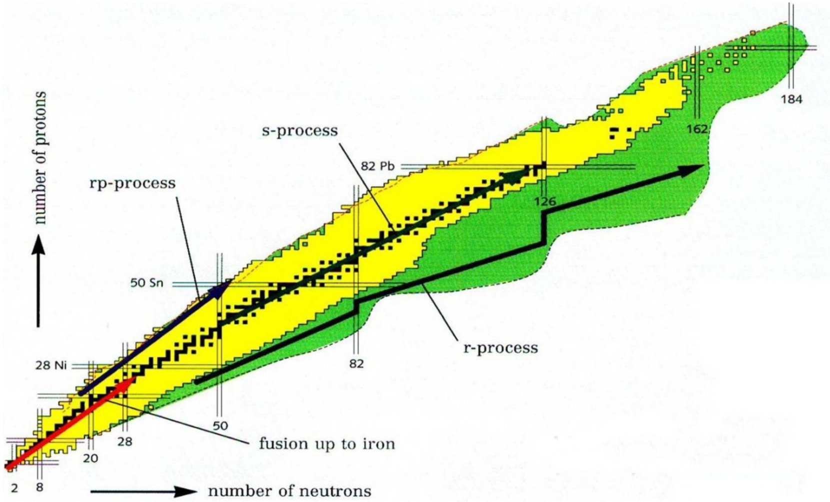

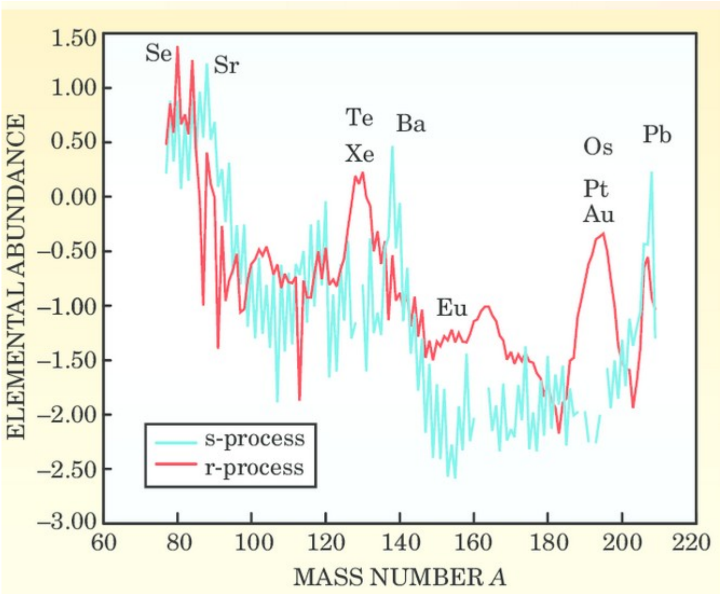

Cowan, John J. et. al. Physics Today (2004)

Physical magnitudes of interest for r-process simulations:

- Half-life ($T_{1/2}$)
- Beta-delayed neutron emission probabilities (P_{xn})
- Masses
- Neutron capture rates
- ...

β-delayed neutron emission

Neutron rich nuclei typically decay via β^-. The energy available for this process is the **Q_β value**. For very rich neutron nuclei the **Q_β** is big enough **($Q_\beta > S_n$)** to allow neutron emission following a β^- decay.
This process is known as **β-delayed** neutron emission.

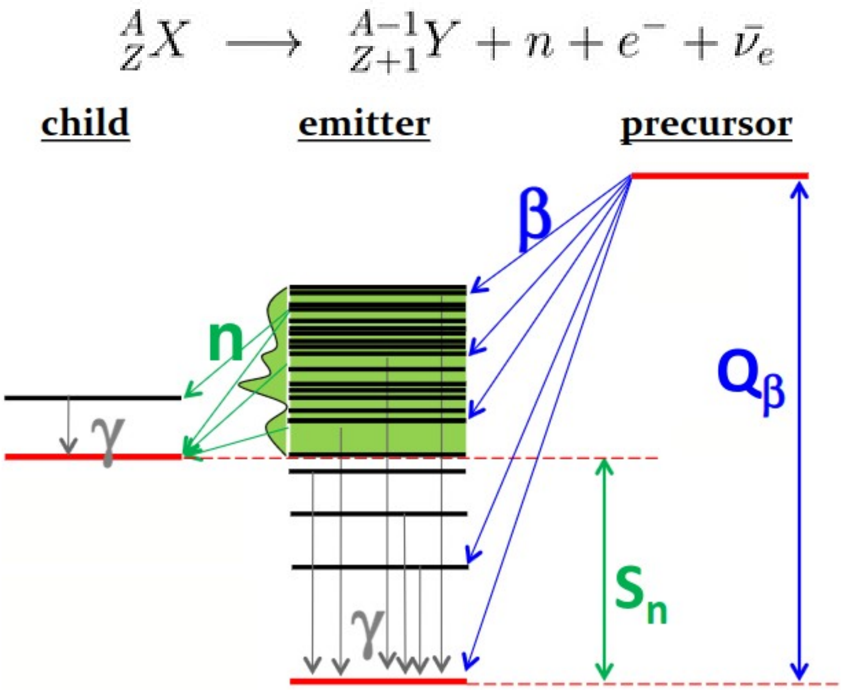

Sabrina Strauss. Stewardship Science Annual Review (2016)

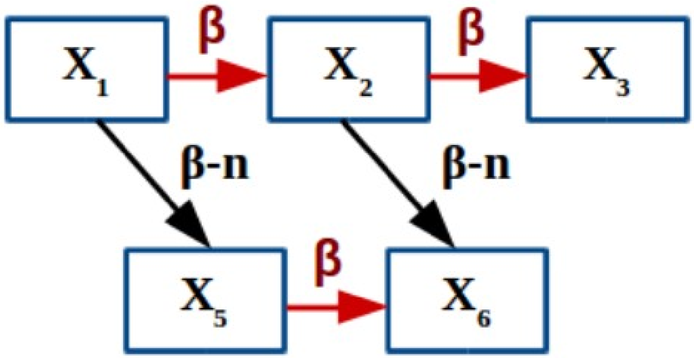

β-delayed neutron emission on REP

According to theoretical models and sensitivity studies, $T_{1/2}$ and P_n of very neutron-rich nuclei for $55 \leq Z \leq 64$ are the most influential ones on the formation of the REP.

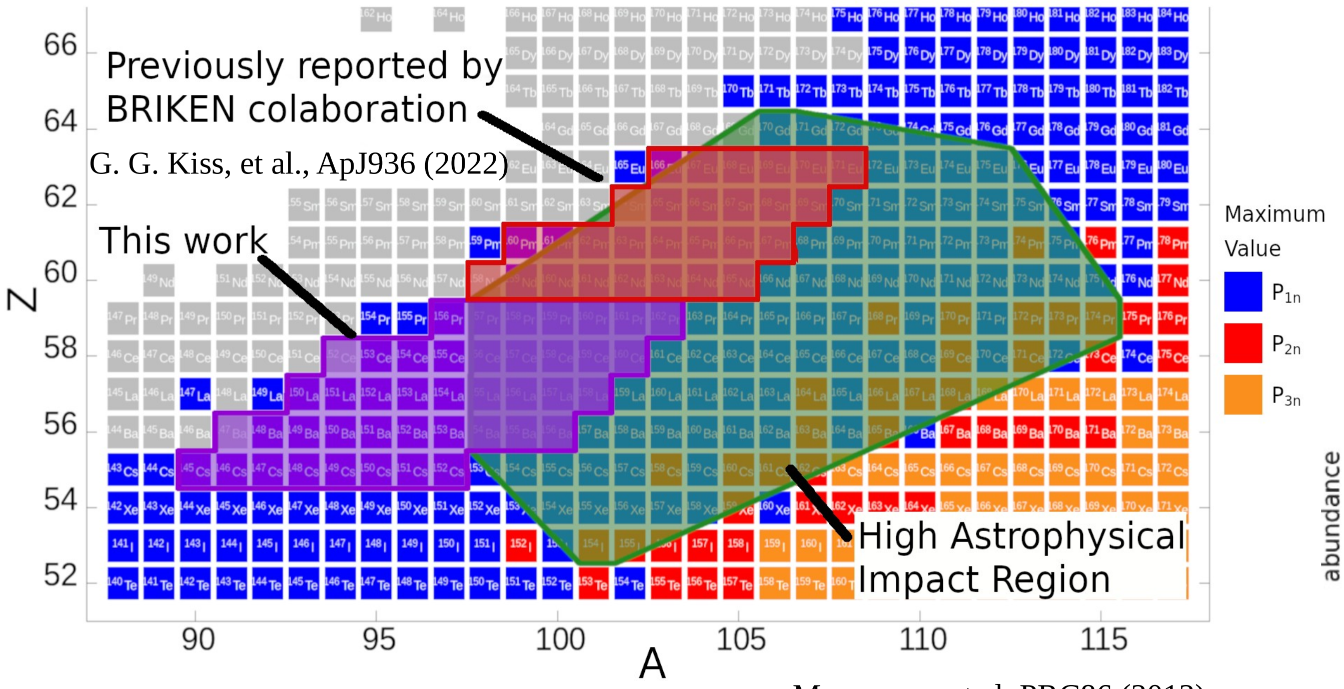

Mumpower et al, PRC86 (2012)

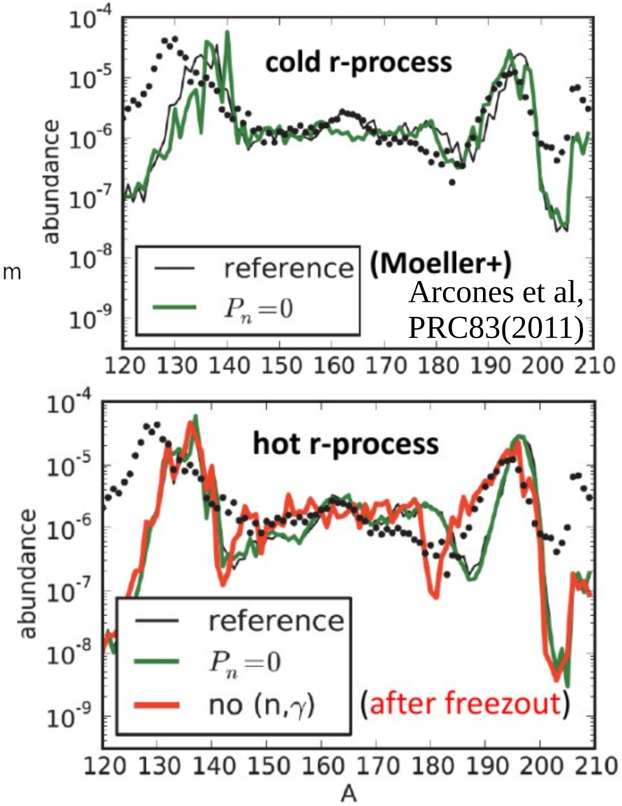

Arcones et al, PRC83(2011)

BRIKEN project

- Riken Nishima Center (Japan).
- The largest beta-delayed detector in the world.
- More than 50 participants from 18 international institutions
- Aims to study very rich neutron isotopes characterized by their:
  - Half-life ($T_{1/2}$)
  - Emission probabilities (P_{xn})

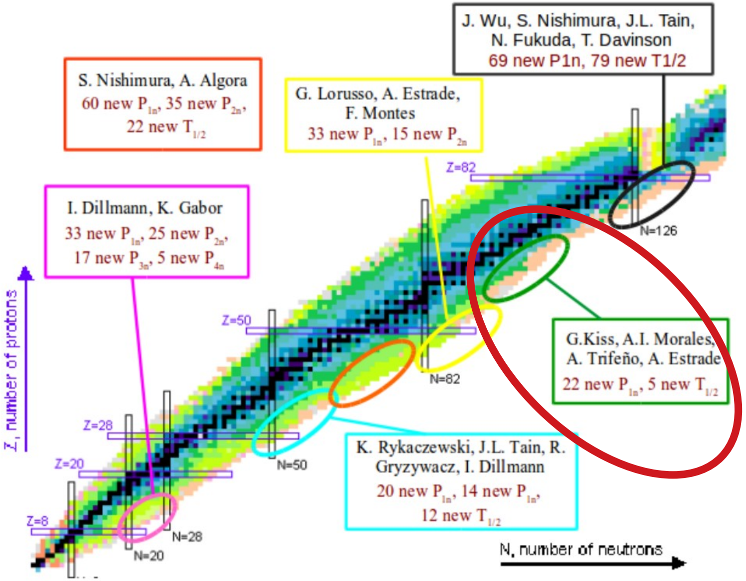

	Identified (Qbxn>0) # of isotopes	Measured (06/2017) # of isotopes	Fraction	Measured mass region
β1n	621	298	48.0%	^{8}He-^{216}Tl
β2n	300	23	7.7%	^{11}Li-^{136}Sb
β3n	138	4	2.9%	^{11}Li-^{31}Na
β4n	58	1	1.7%	^{17}B

Index

Experimental setup

This experimental setup is composed of:

1. BigRIPS+ZeroDegree fragment separators

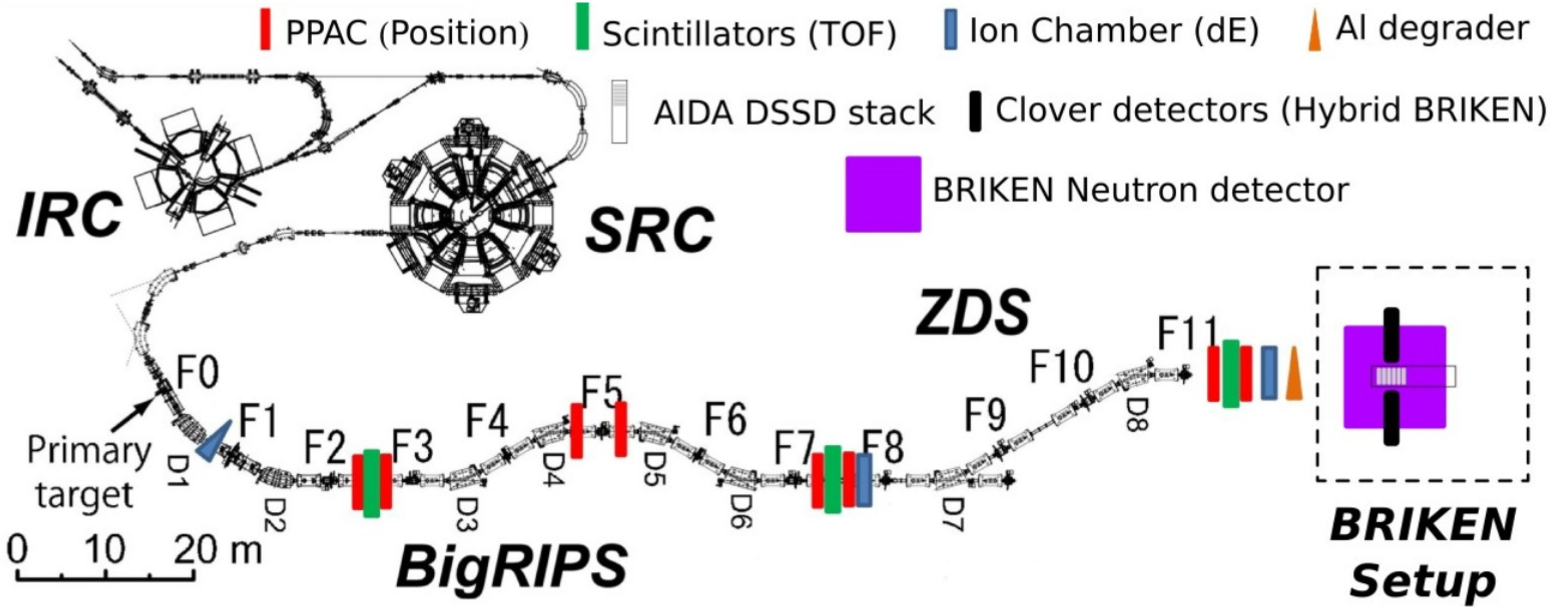

Experimental setup

This experimental setup is composed of:

1. BigRIPS+ZeroDegree fragment separators
2. Advanced Implantation Detector Array (AIDA)
   - Stack of 6 silicon double-sided detectors.

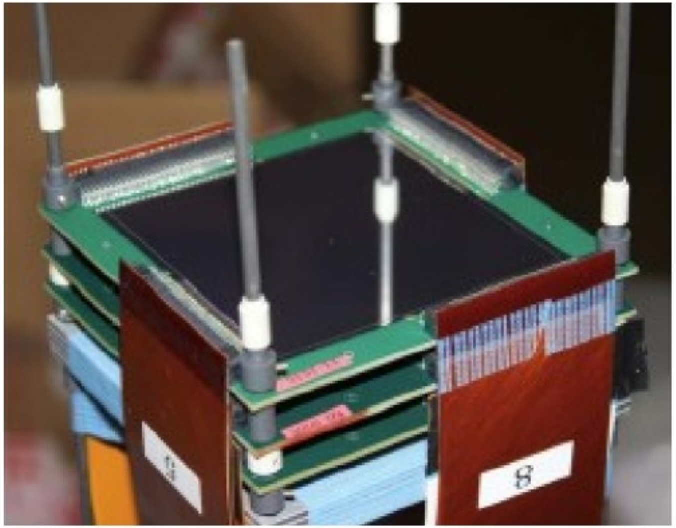

Griffin et al, PoS(NIC XIII)097 2015

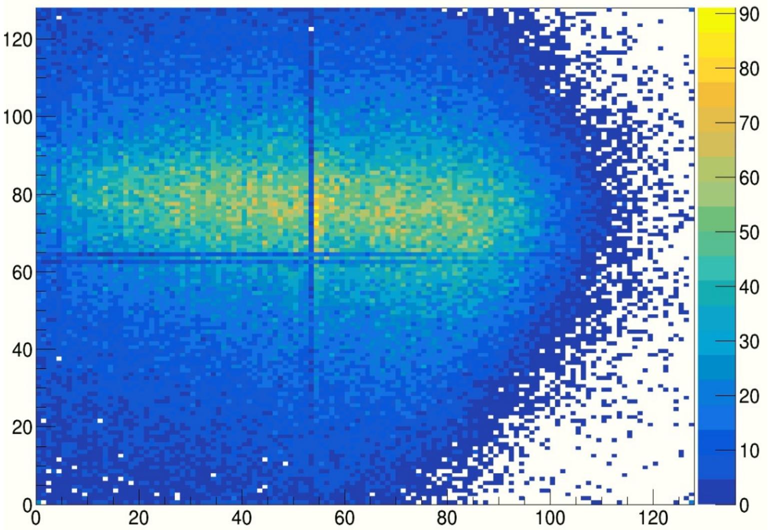

Experimental setup

This experimental setup is composed of:

1. BigRIPS+ZeroDegree fragment separators
2. Advanced Implantation Detector Array (AIDA)
    - Stack of 6 silicon double-sided detectors.
3. BRIKEN detector
    - 140 ^{3}He tubes + HDPE moderator for neutron detection.
    - 2 Clover type HPGe gamma detectors.
    - Ancillary (F11, Si…).

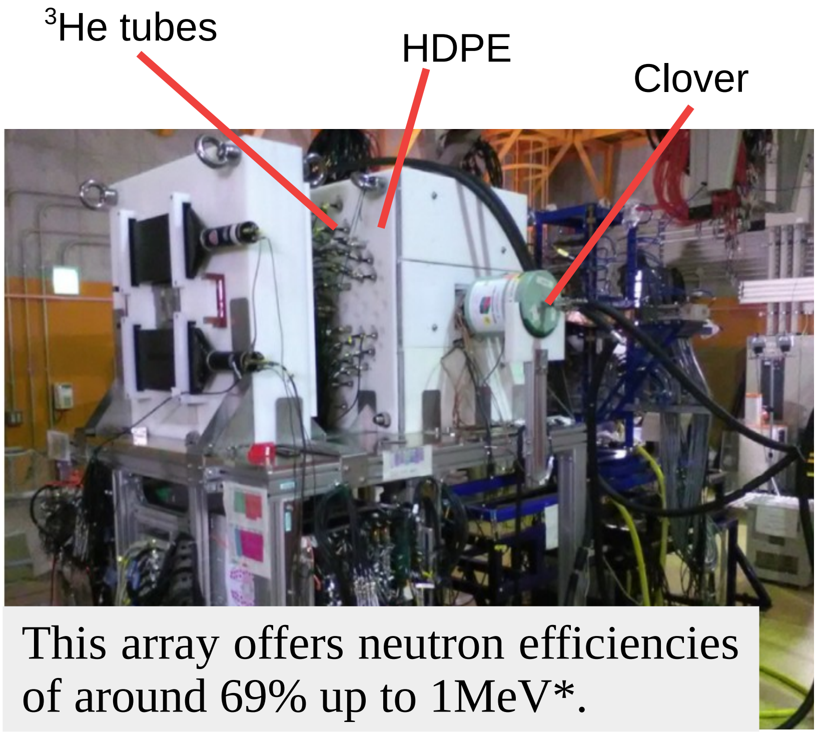

This array offers neutron efficiencies of around 69% up to 1MeV*.

A. Tarifeño-Saldivia et. al. J. Instrum. (2017).

*M. Pallas et. al. ArXiv:2204.13379 (2022)
Full report to be submited (2023).

Index

Experimental data

- The data used in this analysis came from an experiment conducted by the BRIKEN Collaboration in October 2018 at RIBF RIKEN.
- In the 2018 experimental run, a **60-particle-nA 238U beam**, with **345 MeV/nucleon**, hitting a **4 mm thick Be target** was used to produce the secondary radioactive beam. The neutron-rich fragments were filtered out by the BigRIPS fragment separator.
- **108 hours** of measures were analyzed. In this study, we rerport the results isotopes from Ba to Nd.

Data Analysis

1. Acquisition is run by three different DAQs (BigRIPS, AIDA and BRIKEN). To ensure syncronization, a signal is fed to each DAQ.
2. Data is merged into a single file where temporal correlation vectors are built.

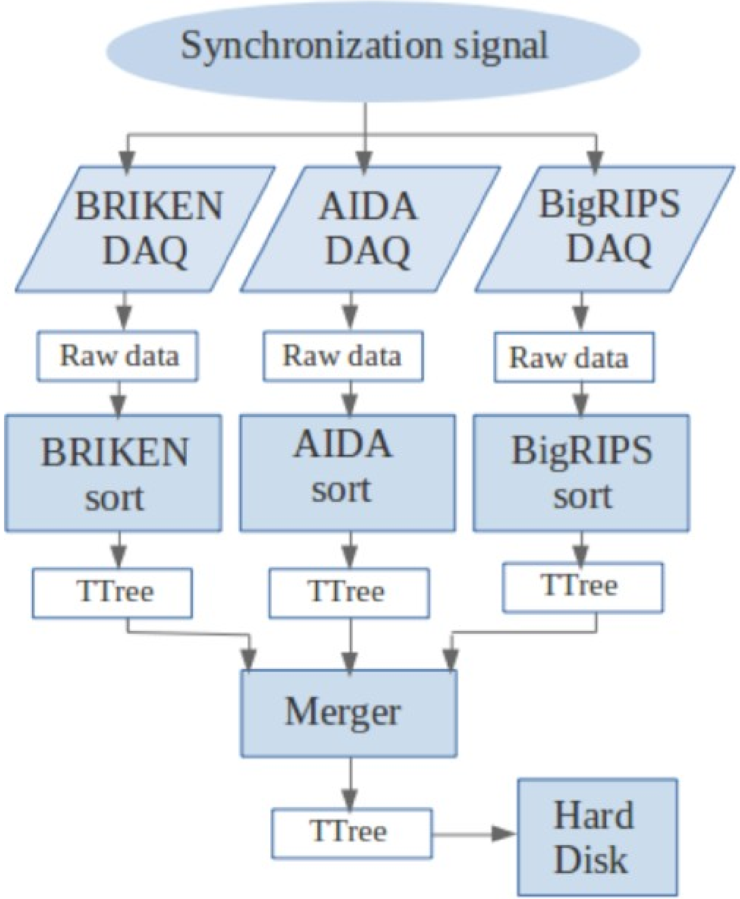

Data Analysis

1. Acquisition is run by three different DAQs (BigRIPS, AIDA and BRIKEN). To ensure syncronization, a signal is fed to each DAQ.
2. Data is merged into a single file where temporal correlation vectors are built.
3. Sort the merged data to obtain β-implant ($T_{i\beta}$) and β-implant-neutron ($T_{i\beta n}$) time correlation histograms for each isotope.

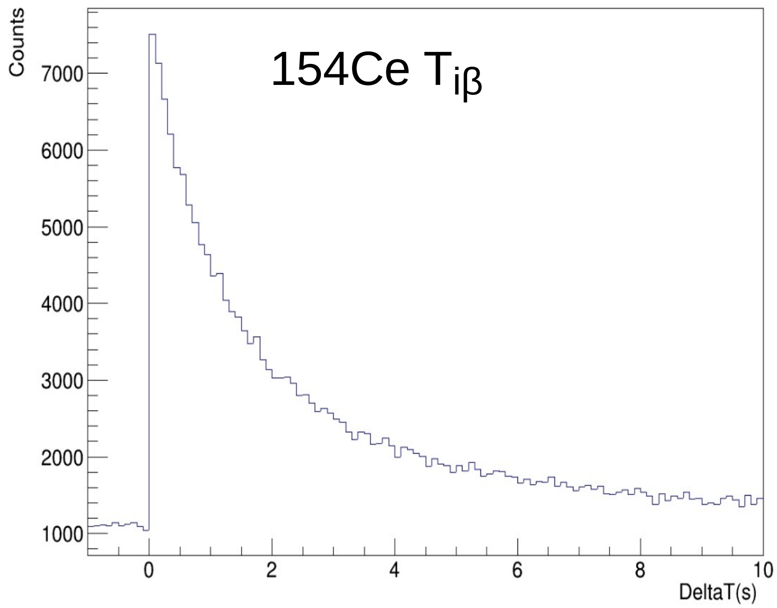

Data Analysis

1. Acquisition is run by three different DAQs (BigRIPS, AIDA and BRIKEN). To ensure syncronization, a signal is fed to each DAQ.
2. Data is merged into a single file where temporal correlation vectors are built.
3. Sort the merged data to obtain β-implant ($T_{i\beta}$) and β-implant-neutron ($T_{i\beta n}$) time correlation histograms for each isotope.
4. $T_{1/2}$ and P_{1n} values are obtained from the simultaneous fit of these histograms.

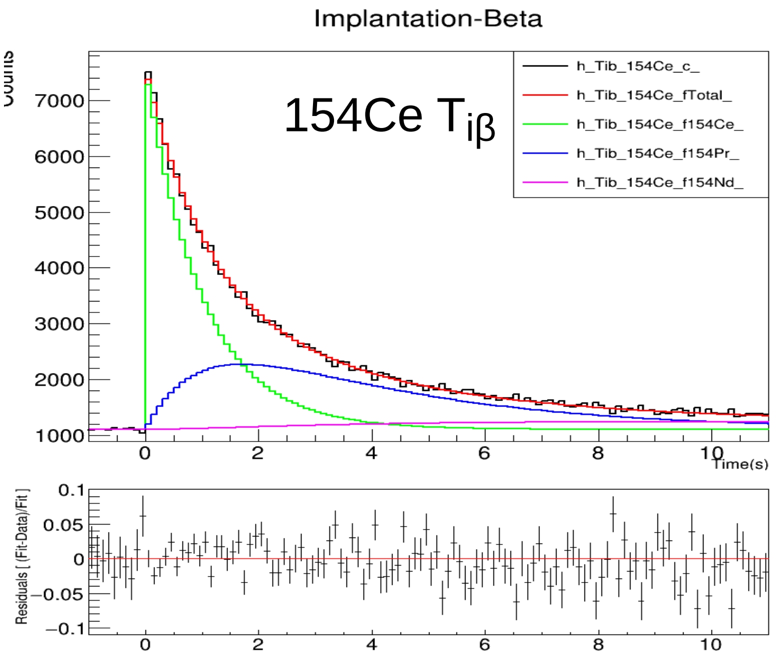

Fitting procedure

After obtaining the time-correlated histograms, we perform a self-consistent fitting procedure* to obtain $T_{1/2}$ and P_{1n} values using Bateman equations.

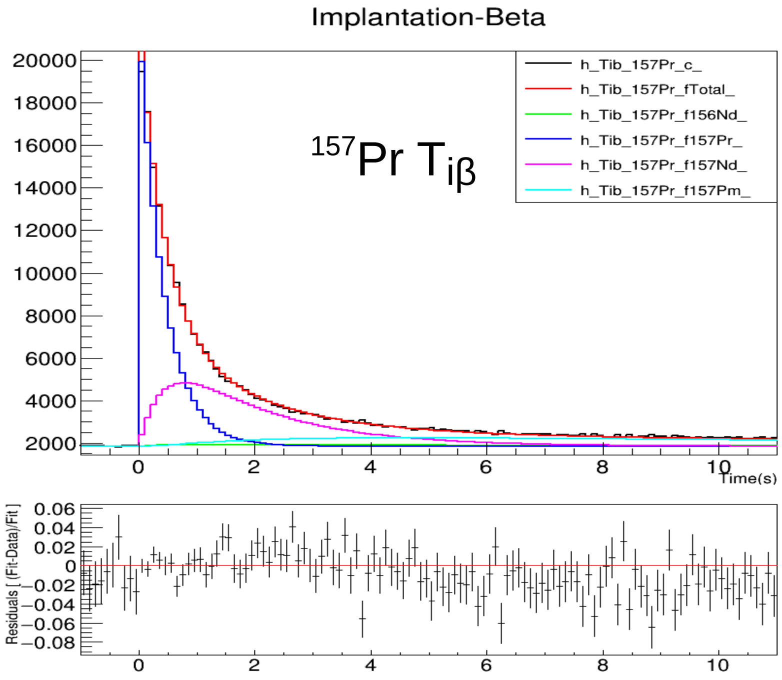

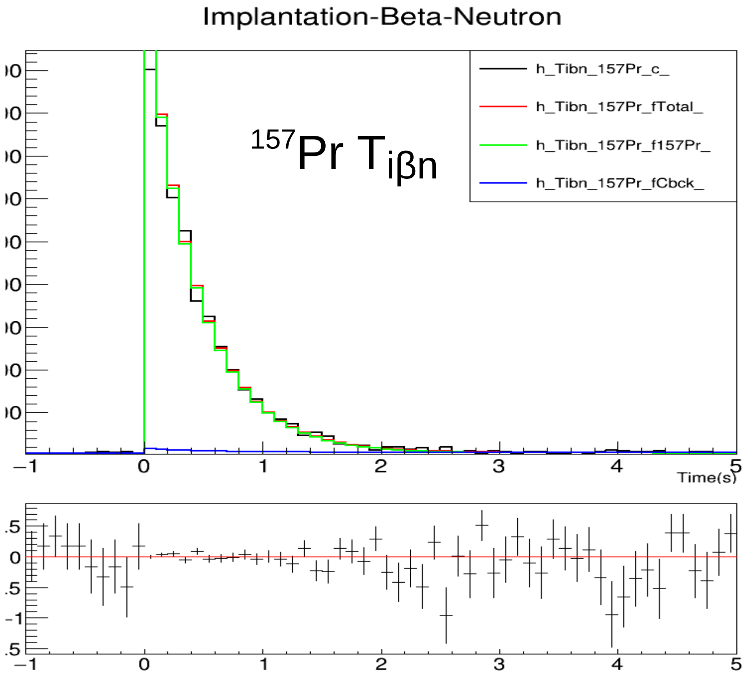

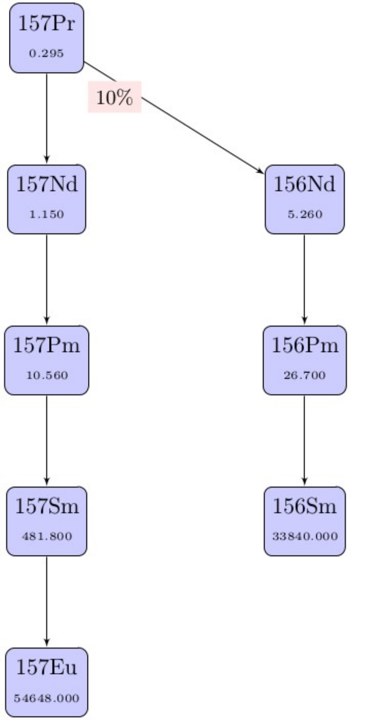

*A. Tolosa-Delgado et al. NIM A 925 (2019) 133-147

Index

Particle identification

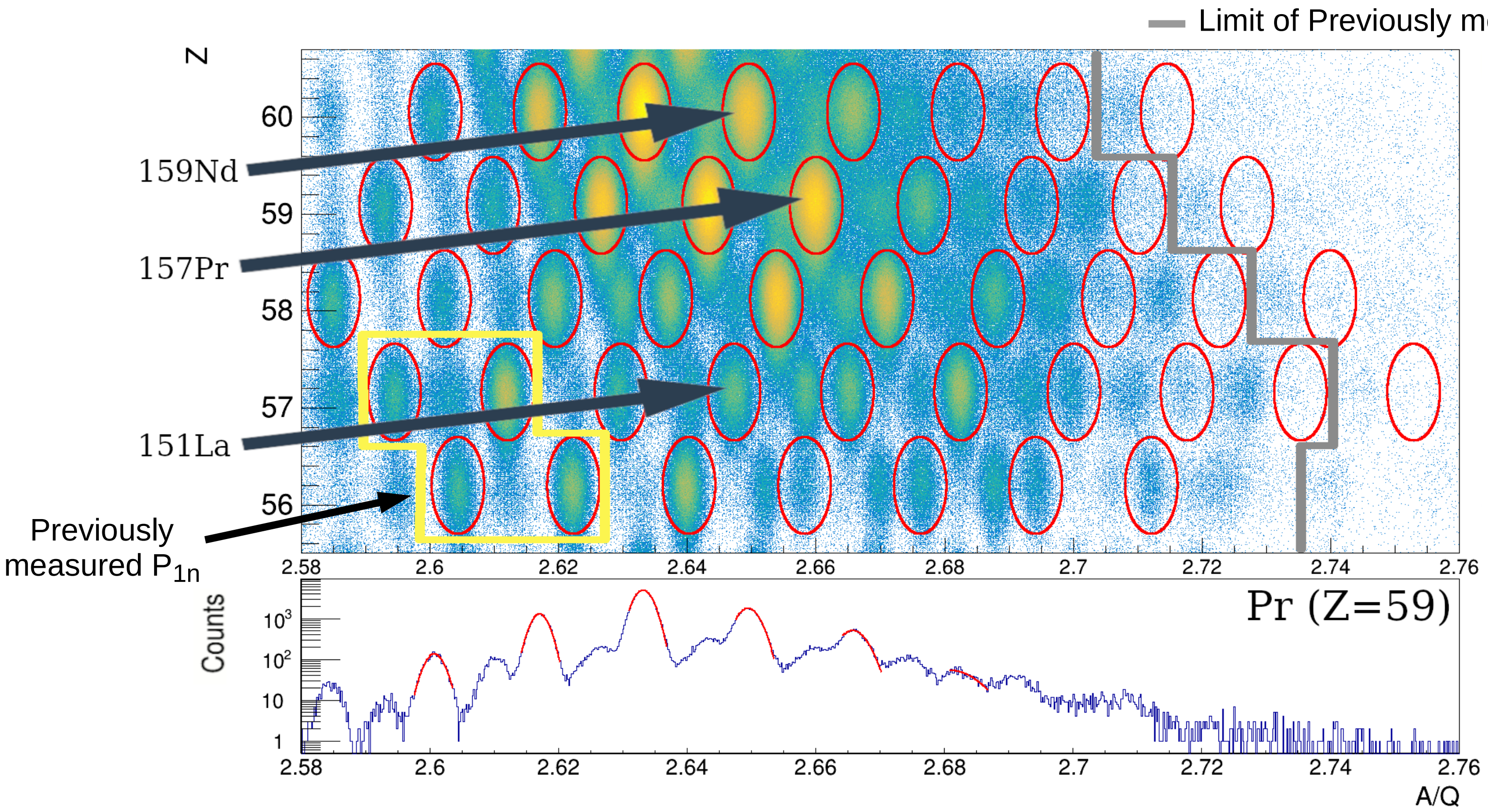

*J. Wu et al. Phys. Rev. Lett. 118-7 (2017)

$T_{1/2}$ results

- Consistent results with previous measurements. **34 $T_{1/2}$ values** have been remeasured many with improved precision.
- Additionally, we report **1 new $T_{1/2}$**.
- New higher limits will be presented in the final report.

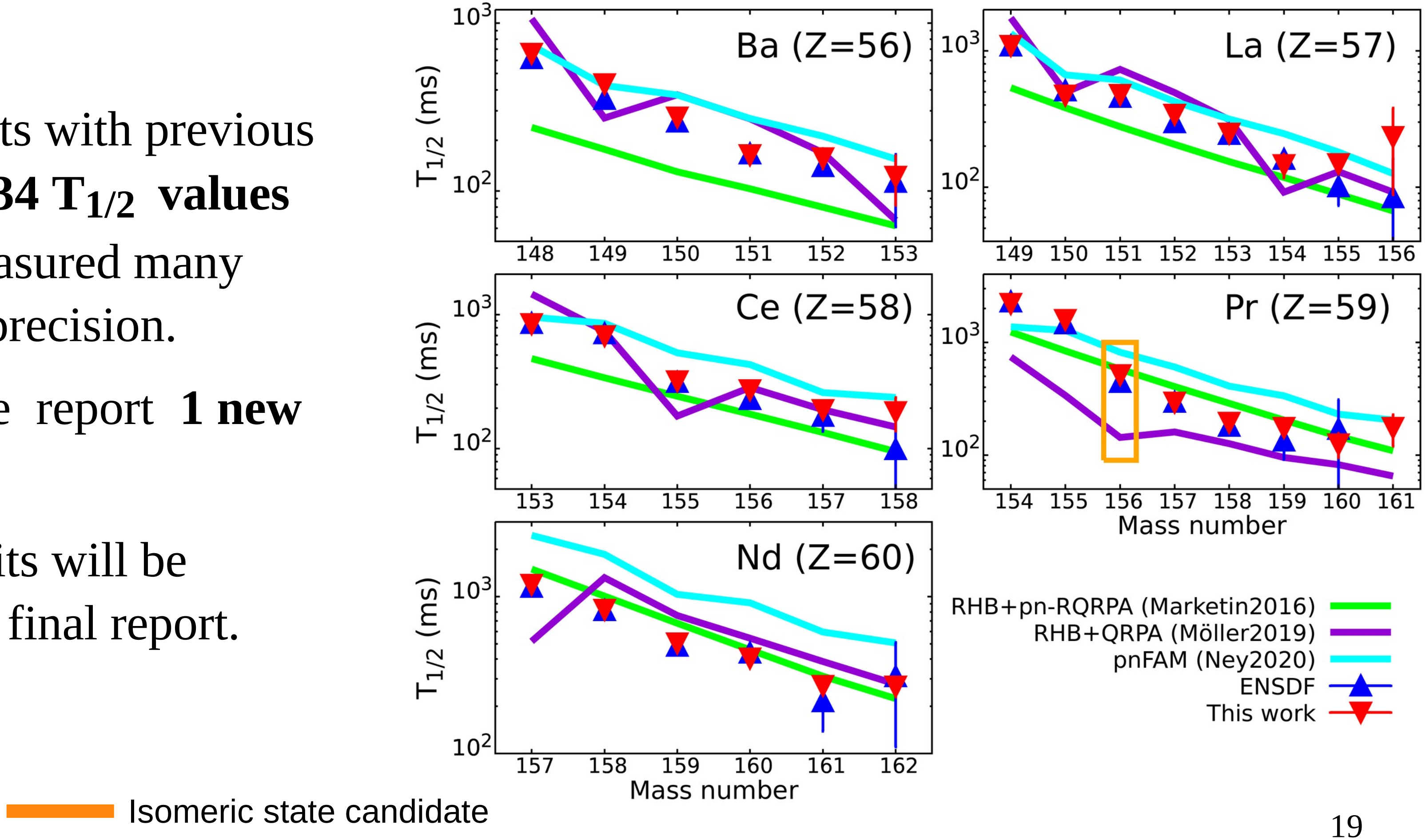

P_{1n} results

- **20 new P_{1n} values** reported.
- **2 P_{1n} values** have been remeasured with improved precision.
- New higher limits will be presented in the final report.

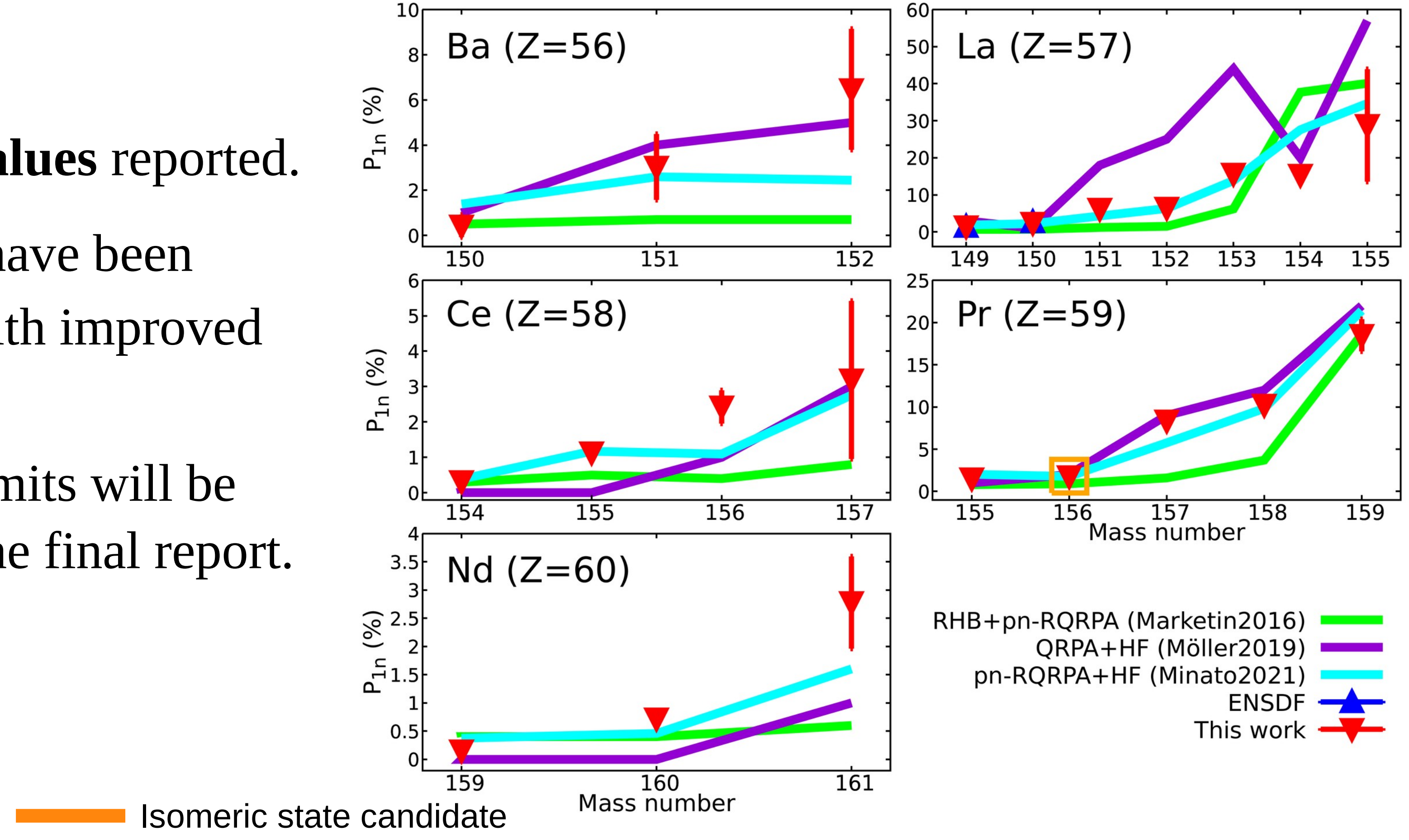

P_{1n} results

- **20 new P_{1n} values** reported.
- **2 P_{1n} values** have been remeasured with improved precision.
- New higher limits will be presented in the final report.

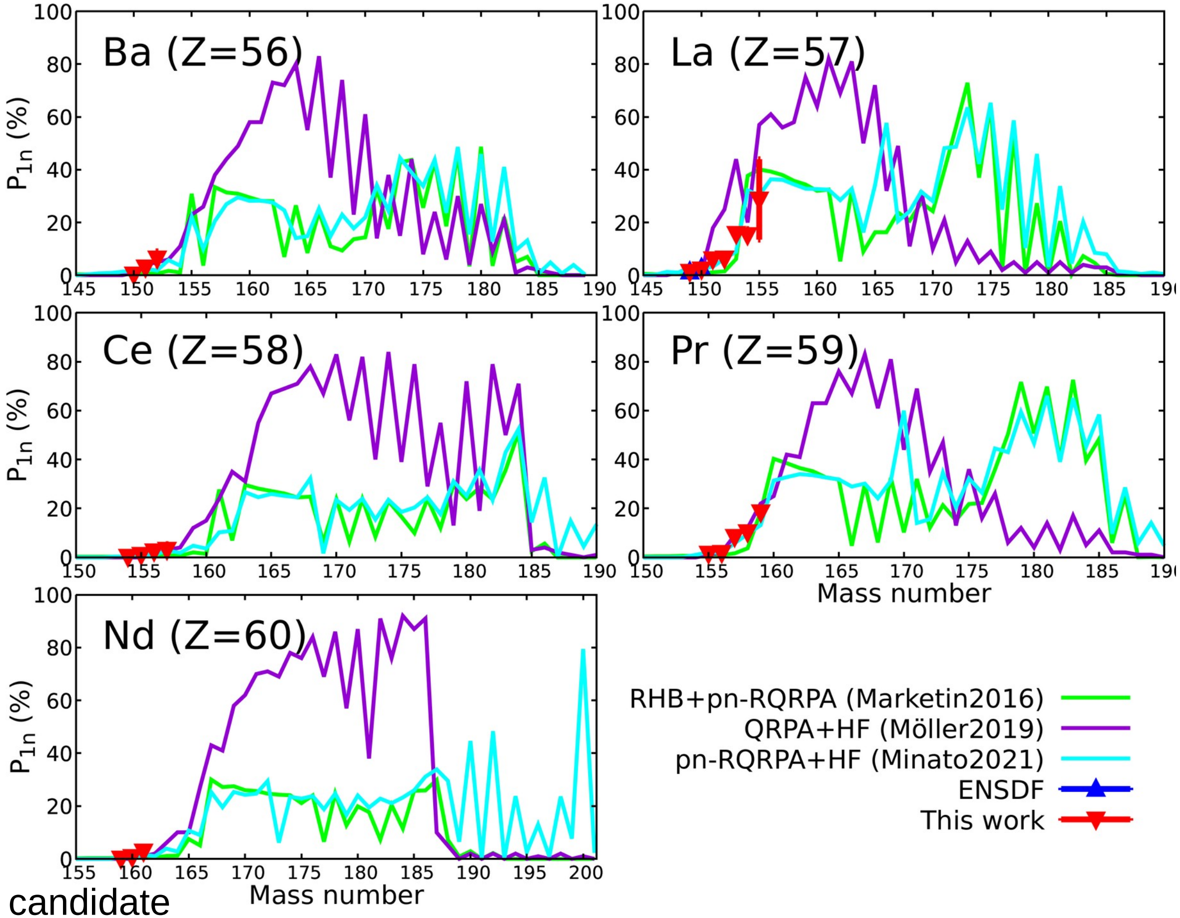

Isomeric state candidate

Remarks

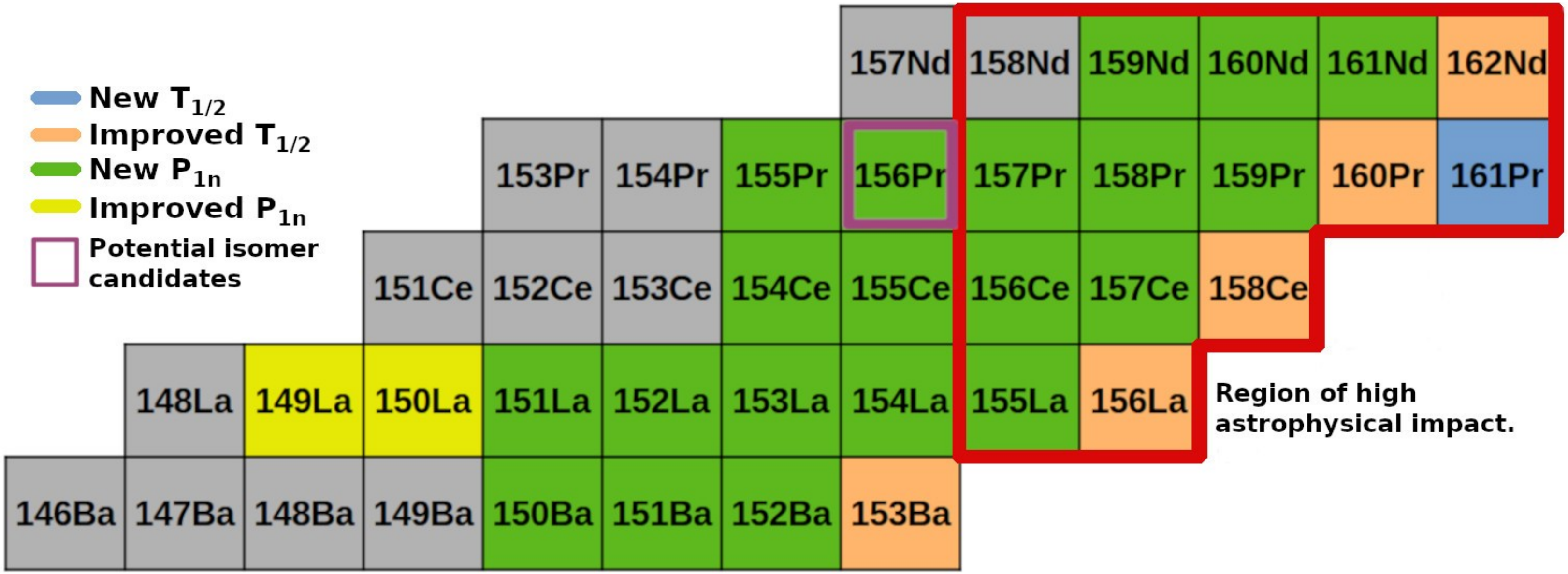

Next steps:

1. Finish the systematic errors evaluation.
2. Astrophysical impact of the new data on the description of the r-process.

Acknowledgments

M. Pallàs[1*], A. Tarifeño-Saldivia[2,1†], G. G. Kiss[3], J. L. Tain[2], A. Tolosa-Delgado[5,2], A. Vitéz-Sveiczer[3,4], F. Calviño[1], J. Agramunt[2], P. Aguilera[6], A. Algora[2], J. M. Allmond[7], H. Baba[8], N. T. Brewer[9,7], R. Caballero-Folch[10], P. J. Coleman-Smith[11], G. Cortes[1], T. Davinson[12], I. Dillmann[10,13], C. Domingo-Pardo[2], A. Estrade[14], N. Fukuda[8], S. Go[15,16], C. J. Griffin[10], R. K. Grzywacz[9,7], O. Hall[12], L. J. Harkness-Brennan[17], T. Isobe[8], D. Kahl[12], T. T. King[9], A. Korgul[18], S. Kovács[4], S. Kubono[8], M. Labiche[11], J. Liu[19], M. Madurga[9], K. Miernik[18], F. Molina[6], N. Mont-Geli[1], A. I. Morales[2], E. Nácher[2], A. Navarro[1], N. Nepal[8], S. Nishimura[8], M. Piersa-Silkowska[18], V. Phong[8], B. C. Rasco[9,7], J. Romero-Barrientos[6], B. Rubio[2], K. P. Rykaczewski[7], Y. Saito[10,20], H. Sakurai[8], Y. Shimizu[8], M. Singh[9], T. Sumikama[8], H. Suzuki[8], T. N. Szegedi[3], H. Takeda[8], K. Wang[14], M. Wolińska-Cichocka[21], P. J. Woods[12], and R. Yokoyama[16] for the BRIKEN collaboration[22]

[1]Institut de Tècniques Energètiques (INTE), Universitat Politècnica de Catalunya (UPC), 08028 Barcelona, Spain.
[2]Instituto de Física Corpuscular (IFIC), CSIC-UV, E-46980 Paterna, Spain.
[3]Institute for Nuclear Research (ATOMKI), 4026 Debrecen, Bem tér 18/c, Hungary.
[4]University of Debrecen, 4032 Debrecen, Egyetem tér 1, Hungary.
[5]Department of Physics, University of Jyväskylä, Finland.
[6]Centro de Investigación en Física Nuclear y Espectroscopía de Neutrones (CEFNEN). Comisión Chilena de Energía Nuclear, Nueva Bilbao 12501, Las Condes, Santiago-Chile.
[7]Physics Division, Oak Ridge National Laboratory, Oak Ridge, TN 37830, USA.
[8]RIKEN Nishina Center, 2-1 Hirosawa, Wako, Saitama 351-0198, Japan.
[9]Department of Physics and Astronomy, University of Tennessee, Knoxville, Tennessee 37996, USA.
[10]TRIUMF, 4004 Wesbrook Mall, Vancouver, BC V6T 2A3, Canada.
[11]STFC Daresbury Laboratory, Daresbury, Warrington WA4 4AD, United Kingdom.
[12]School of Physics and Astronomy, The University of Edinburgh, Edinburgh EH9 3FD, United Kingdom.
[13]Department of Physics and Astronomy, University of Victoria, Victoria, BC V8P 5C2, Canada.
[14]Central Michigan University, Mt. Pleasant, MI 48859, USA.
[15]Department of Physics, Kyushu University, 744 Motooka, Fukuoka 819-0395, Japan.
[16]Center for Nuclear Study, The University of Tokyo, 2-1 Hirosawa, Wako, Saitama 351-0106, Japan.
[17]Department of Physics, University of Liverpool, Liverpool L69 7ZE, United Kingdom.
[18]Faculty of Physics, University of Warsaw, 02-093 Warsaw, Poland.
[19]Department of Physics, the University of Hong Kong, Pokfulam Road, Hong Kong.
[20]Department of Physics and Astronomy, The University of British Columbia, Vancouver BC V6T 1Z1, Canada.
[21]Heavy Ion Laboratory, University of Warsaw, Pasteura 5A, 02-093 Warsaw, Poland.

Backup

$T_{1/2}$ model comparison

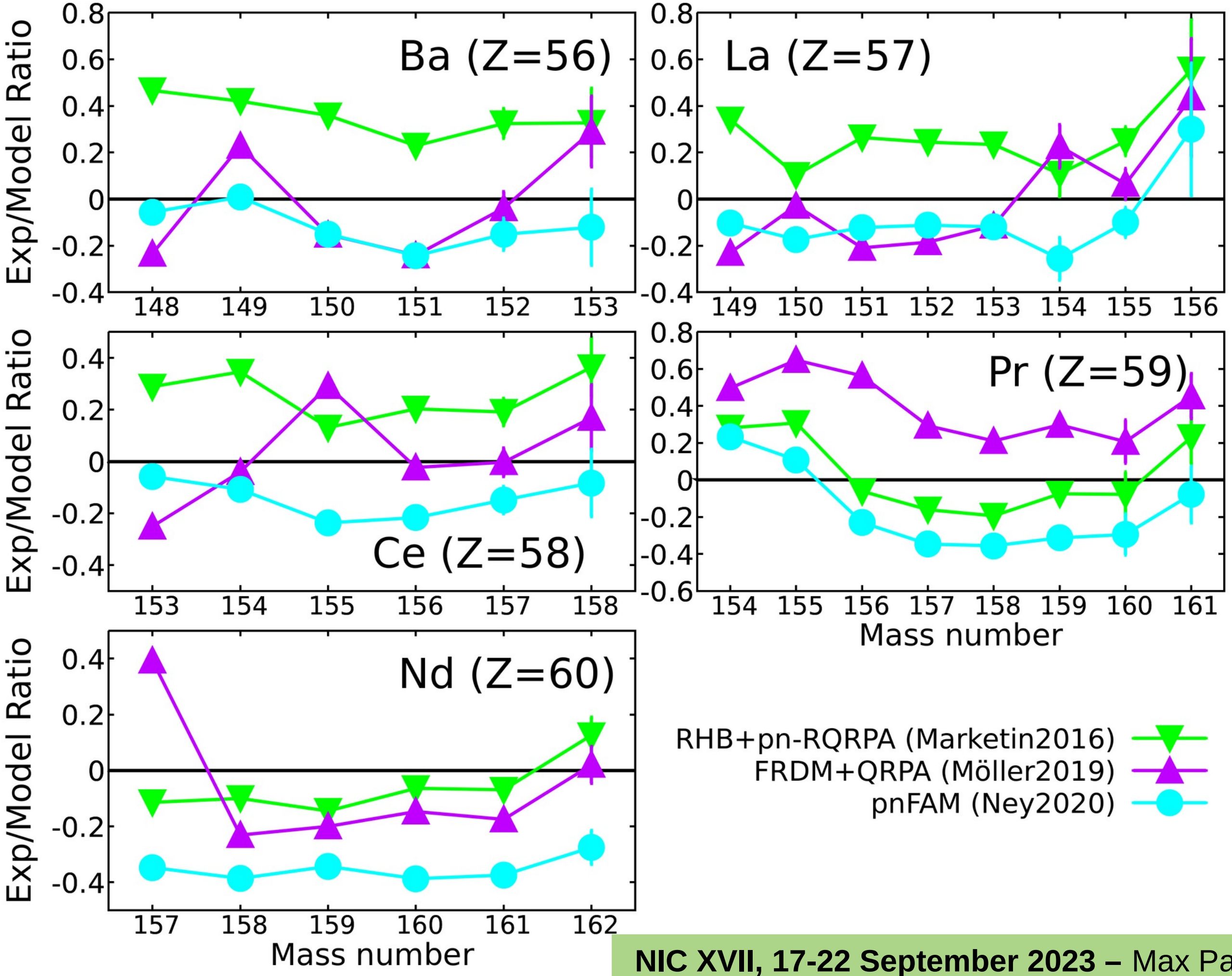

P_{1n} model comparison

Overall pn-RQRPA+HF (Minato2021) fits our data the best. In particular for La isotopes.

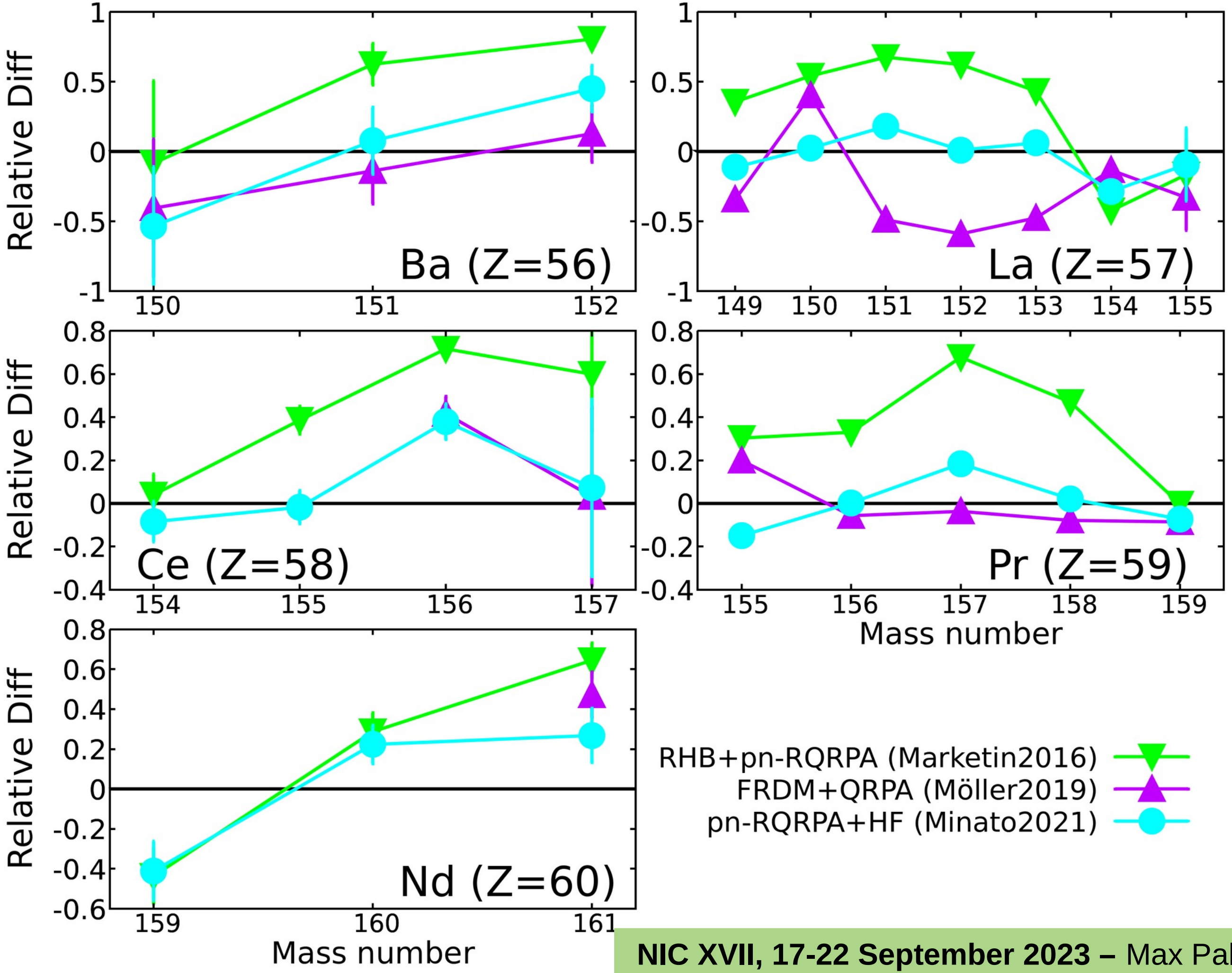

Improve signal to noise ratio

The are multiple techniques to reduce the background of our measures and improve the signal to noise ratio:

- Beta veto window using ancillary detectors.

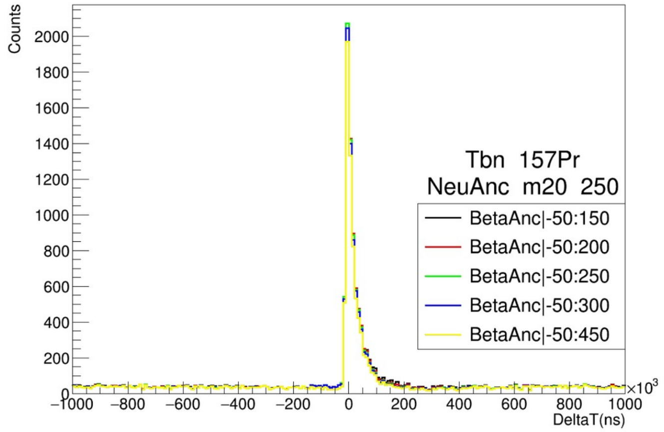

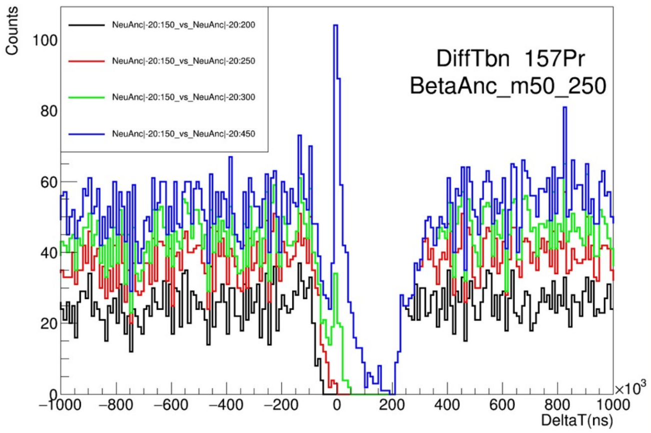

Improve signal to noise ratio

The are multiple techniques to reduce the background of our measures and improve the signal to noise ratio:

- Beta veto window using ancillary detectors.
- Neutron veto window using ancillary detectors (only affects $T_{i\beta n}$).

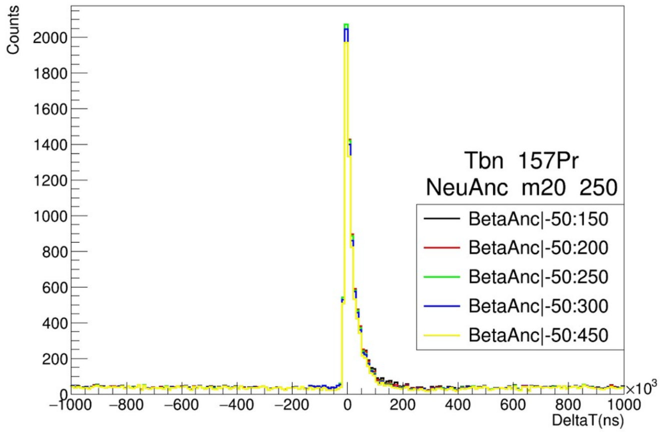

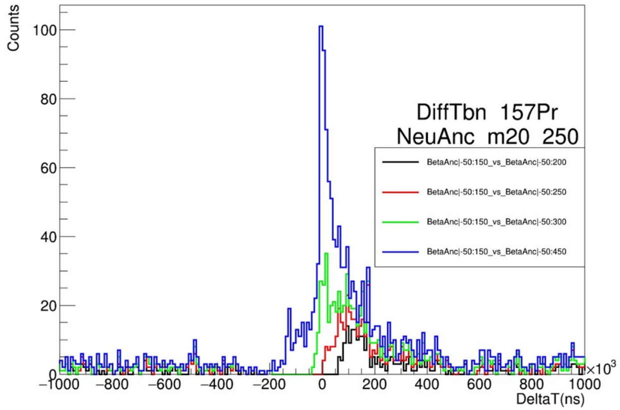

Improve signal to noise ratio

The are multiple techniques to reduce the background of our measures and improve the signal to noise ratio:

- Beta veto window using ancillary detectors.
- Neutron veto window using ancillary detectors (only affects $T_{i\beta n}$).
- Beta energy threshold

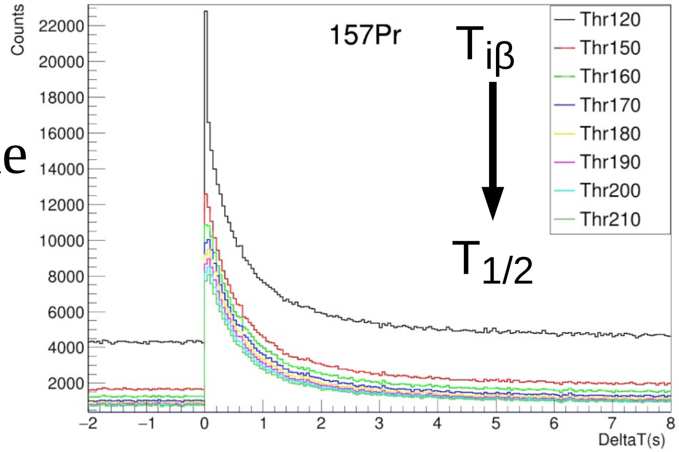

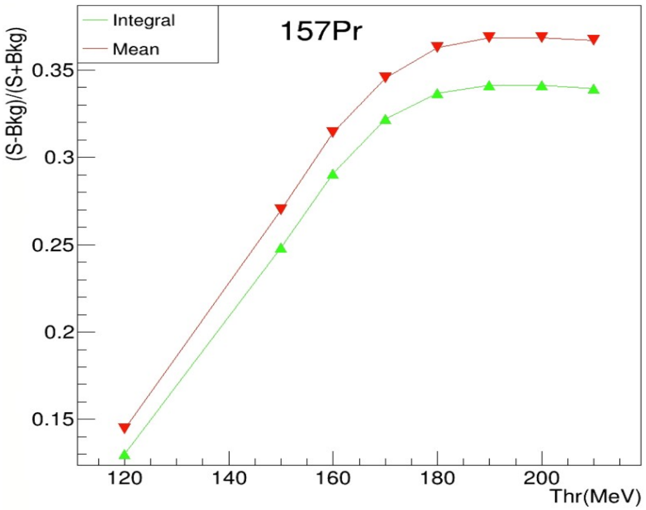

Fix charged states

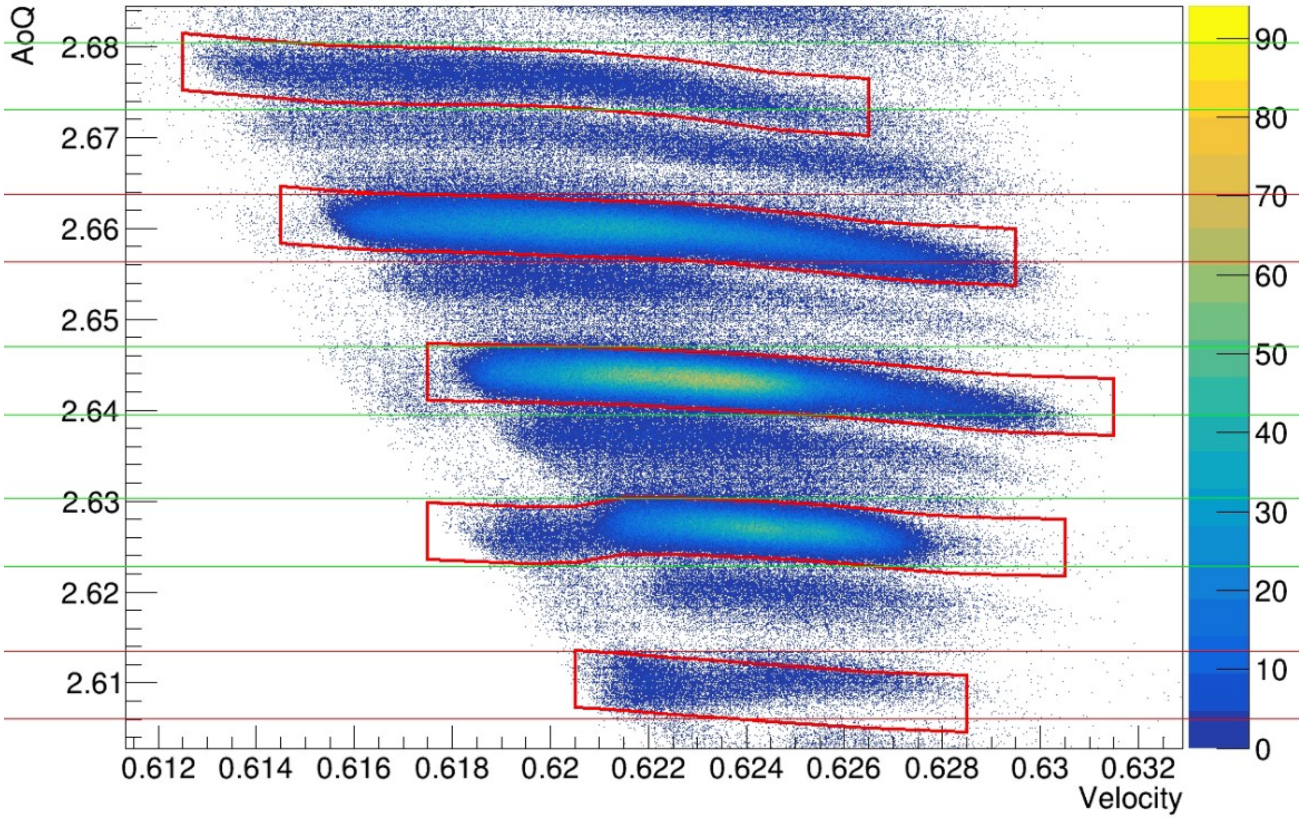

Theoretical models

RHB+pn-RQRPA: Relativistic Hartree Bogoliubov + proton-neutron Relativistic Quasiparticle Random Phase Approximation

QRPA+HF: Quasiparticle Random-Phase Approximation + Hauser-Feshbach

pnFAM: proton-neutron Finite Amplitude Method

pn-RQRPA + HF: proton-neutron Relativistic Quasiparticle Random-Phase Approximation + Hauser-Feshbach statistical model

Isomer effect

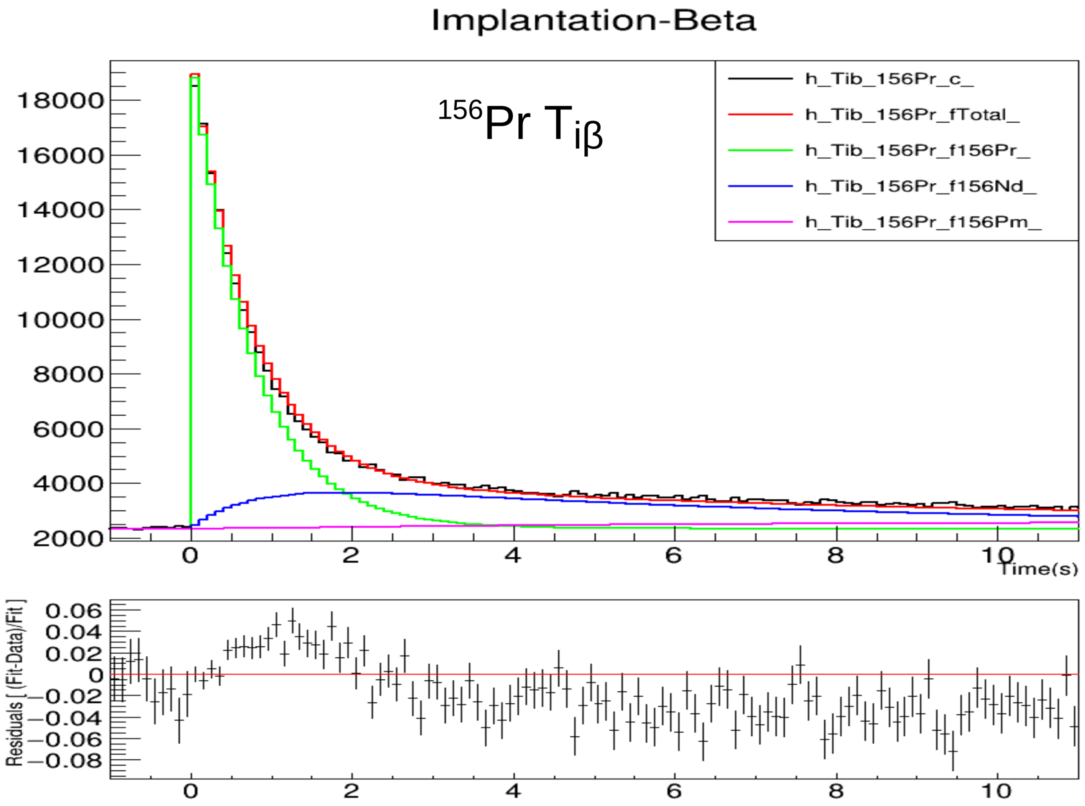

BRIKEN detector

This detector is composed of:

1. 140 ^{3}He tubes for neutron detection.
2. 2 Clover type HPGe gamma detectors.
3. Ancillary (F11, Si…).
4. HDPE moderator and shielding.

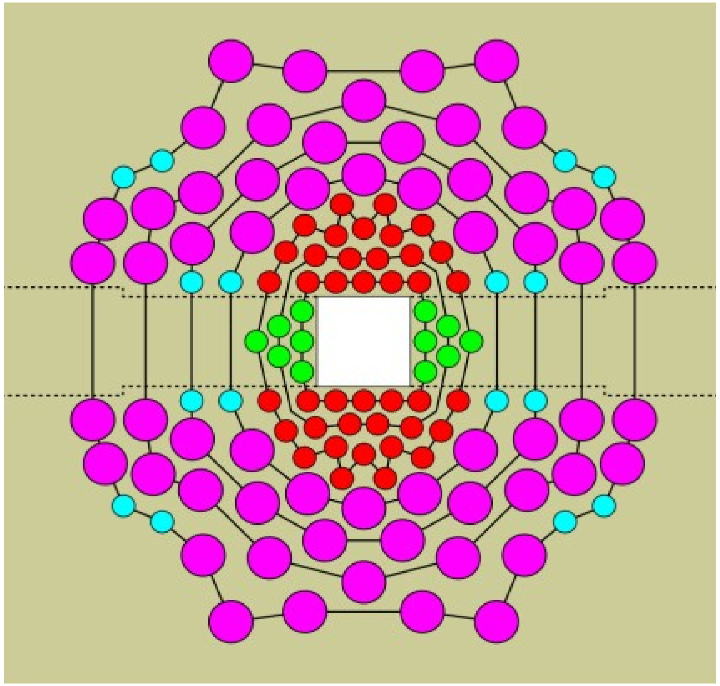

Design: A. Tarifeño-Saldivia et. al. Journal of Instrumentation, 12(04):P04006–P04006, apr 2017.

BRIKEN detector

This detector is composed of:

1. 140 ^{3}He tubes for neutron detection.
2. 2 Clover type HPGe gamma detectors.
3. Ancillary (F11, Si…).
4. HDPE moderator and shielding.

This array offers neutron efficiencies of around 68.6% up to 1MeV. The expected neutron energy spectra from beta-delayed emission is expected to be below 1MeV.

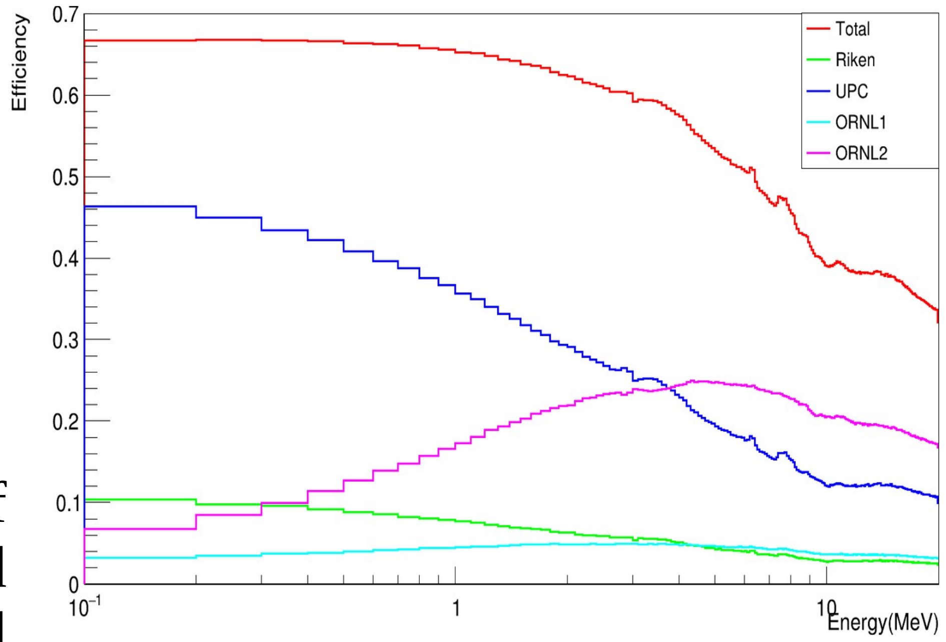

*Characterization of the BRIKEN neutron counter:
M. Pallas et. al. ArXiv:2204.13379 (2022)
Full report to be summited (2023).

$Q_{\beta\text{-}n}$

155Nd -2.08E+3	156Nd -1.33E+3	157Nd -3.98E+2	158Nd 3.90E+2	159Nd 1.31E+3	160Nd 1.75E+3	161Nd 2.59E+3	162Nd 3.00E+3	163Nd 3.88E+3
154Pr 1.39E+3	155Pr 2.09E+3	156Pr 2.76E+3	157Pr 3.69E+3	158Pr 4.27E+3	159Pr 4.99E+3	160Pr 5.45E+3	161Pr 6.16E+3	
153Ce 7.77E+2	154Ce 1.27E+3	155Ce 2.00E+3	156Ce 2.52E+3	157Ce 3.44E+3	158Ce 3.82E+3	159Ce 4.73E+3		
152La 3.86E+3	153La 4.84E+3	154La 5.30E+3	155La 6.21E+3	156La 6.65E+3	157La 7.67E+3			
151Ba 3.30E+3	152Ba 3.62E+3	153Ba 4.74E+3	154Ba 5.06E+3					

$Q_{\beta\text{-}2n}$

4	155Nd -7.77E+3	156Nd -8.07E+3	157Nd -5.69E+3	158Nd -5.81E+3	159Nd -3.56E+3	160Nd -3.76E+3	161Nd 1.01E+3	162Nd -2.25E+3	163Nd -1.36E+2
3	154Pr -3.85E+3	155Pr -4.22E+3	156Pr -2.01E+3	157Pr -2.29E+3	158Pr -9.05E+1	159Pr -4.18E+2	160Pr 1.49E+3	161Pr 1.09E+3	
3	153Ce -4.27E+3	154Ce -4.60E+3	155Ce -2.35E+3	156Ce -3.10E+3	157Ce -6.57E+2	158Ce -1.23E+3	159Ce 9.52E+2		
3	152La -5.85E+2	153La -9.77E+2	154La 1.30E+3	155La 8.37E+2	156La 3.02E+3	157La 2.56E+3			
3	151Ba -8.62E+2	152Ba -1.44E+3	153Ba 6.97E+2	154Ba 2.27E+2					